STATISTICS, OPTIMIZATION AND INFORMATION COMPUTING
Stat., Optim. Inf. Comput., Vol. **15**, April 2026, pp 2769–2780.
Published online in International Academic Press (www.IAPress.org)

Analytical Expression of Nonlinear Vibration Analysis of Triple-Walled Carbon Nanotubes

A.Dorathy Cathrine [1], R. Raja[2], R. Swaminathan[1,*]

[1]*PG & Research Department of Mathematics, Vidhyaa Giri College of Arts and Science, (Affiliated to Alagappa University), Puduvayal 630108, Tamil Nadu, India*
[2]*Ramanujan Centre for Higher Mathematics, Alagappa University, Karaikudi, Tamilnadu, India*

Abstract This article employs the homotopy perturbation method (HPM) to derive analytical solutions for the nonlinear vibrations of triple-walled carbon nanotubes (TWCNTs) embedded in an elastic medium. A triple-beam model is used, where the governing equations for each layer are coupled with those of adjacent layers through van der Waals interlayer forces. The study examines the amplitude-frequency response of TWCNTs under large-amplitude vibrations, analysing the effects of variations in the elastic medium's material properties as well as changes in the nanotube's geometric parameters. Using the homotopy perturbation method (HPM), a nonlinear system of equations can be reformulated into an approximate analytical expression. The numerical results demonstrate the rapid convergence of the derived series solutions toward the exact solution. Additionally, the analytical findings are validated against simulation results obtained using a MATLAB program, showing strong agreement between the two approaches.

Keywords Nonlinear vibrations, carbon nanotubes, homotopy perturbation method, nanoscale dynamics, energy transfer

AMS 2010 subject classifications 34A34, 34B15, 34B18, 34B60

DOI: 10.19139/soic-2310-5070-3082

1. Introduction

Carbon nanotubes (CNTs) are among the most transformative breakthroughs in nanotechnology, having been discovered in 1991. Renowned for their remarkable combination of mechanical robustness, electrical conductivity, thermal resilience, and nanoscale geometry, these cylindrical nanostructures—formed by rolling graphene sheets into seamless cylinders—have revolutionised fields ranging from advanced electronics and high-performance composites to energy storage systems and biomedical technologies [1]. Among these nanostructures, triple-walled carbon nanotubes (TWCNTs) occupy a unique position. While single-walled (SWCNTs) and double-walled (DWCNTs) variants have dominated scientific inquiry, TWCNTs bridge the gap between the well-defined electronic properties of single-walled systems and the enhanced structural stability of multi-walled architectures. This intermediate configuration positions TWCNTs as a compelling subject for fundamental research and practical applications, offering a synergistic balance of precision and durability unmatched by their counterparts [2].

Carbon nanotubes are systematically classified by their structural configuration, which consists of concentric graphene layers: single-walled (SWCNTs), double-walled (DWCNTs), and multi-walled (MWCNTs), with multiple nested layers. Within the MWCNT category, triple-walled carbon nanotubes (TWCNTs) stand apart due to their precisely defined tri-layered architecture. The uniform three-walled architecture of TWCNTs enables a synergistic integration of outstanding mechanical robustness, high chemical stability, and precisely

*Correspondence to: R. Swaminathan (Email: swaminathanmath@gmail.com).PG & Research Department of Mathematics, Vidhyaa Giri College of Arts and Science.

ISSN 2310-5070 (online) ISSN 2311-004X (print)

adjustable electronic behaviour. These distinctive properties position TWCNTs as pivotal materials for ground-breaking applications, including high-efficiency Nano electronics, precision sensors, next-generation composite reinforcements, and advanced biomedical technologies [3].

Structurally, TWCNTs exhibit exceptional mechanical robustness that surpasses both SWCNTs and DWCNTs. The triple-layered architecture enhances resistance to buckling and fracture under compressive or tensile loads, positioning them as superior candidates for high-strength composites and nanoscale structural applications [4]. Unlike conventional multi-walled carbon nanotubes (MWCNTs), which typically comprise numerous concentric layers with intricate interlayer dynamics, TWCNTs strike an optimal balance: their three-wall configuration simplifies interlayer interactions while retaining the mechanical advantages of multi-walled systems. This structural predictability, coupled with retained durability, enables precise engineering of TWCNT-based materials without sacrificing performance—a critical advantage in advanced manufacturing and nanotechnology design.

The electrical behaviour of TWCNTs offers a unique versatility rooted in their structural design. Unlike single-walled counterparts, TWCNTs exhibit a layered electronic profile governed by their three concentric walls' distinct chirality and diameter [5]. This configuration enables hybrid electronic properties—where metallic and semiconducting behaviours coexist across different layers—allowing engineers to fine-tune conductivity for applications such as flexible Nano electronics or multifunctional Nano devices. A critical advantage lies in their modular design: the outer wall can be chemically functionalized for integration with polymers, biomolecules, or sensing interfaces, while the inner walls remain pristine, preserving intrinsic electrical performance and structural integrity [6].

TWCNTs are primarily synthesised through established techniques such as arc discharge and laser ablation, with chemical vapour deposition (CVD) emerging as the predominant method for controlled fabrication. CVD enables superior control over growth parameters, facilitating the production of nanotubes with enhanced structural uniformity and reduced defect density compared to alternative approaches [7]. Recent breakthroughs in catalyst engineering and thermal regulation have refined the process, enabling selective synthesis of TWCNTs while suppressing the formation of irregular multi-walled byproducts. Despite these advancements, persistent obstacles in maintaining precise structural consistency and purity—particularly in large-scale production scenarios—remain critical barriers to industrial adoption.

TWCNTs extend their significance beyond fabrication, offering an exemplary platform for probing van der Waals interactions and quantum confinement effects in quasi-one-dimensional geometries. Their inter-wall spacing of approximately 0.34 nanometers—akin to the interlayer distance in graphite—enables subtle coupling between concentric layers, modulating phonon propagation, charge transport dynamics, and mechanical responses [8]. This weak yet consequential interaction framework is essential for elucidating the behaviour of concentric graphene cylinders under diverse physical and chemical perturbations, providing foundational insights into nanoscale material science.

TWCNTs exhibit transformative potential across a spectrum of advanced technologies. Their exceptional mechanical strength and expansive surface area position them as key enhancers for lithium-ion batteries and supercapacitors, significantly boosting energy storage capacity and rapid charge-discharge performance [9]. In biotechnology, their unique architecture—featuring a chemically tunable outer shell and an inert, stable core—enables precise drug delivery mechanisms and high-sensitivity biosensors, ensuring both efficacy and biocompatibility. Beyond these domains, their remarkable thermal management capabilities and resistance to corrosive environments have spurred innovations in aerospace materials and electronics for extreme operational conditions, such as high-temperature circuits and propulsion systems [10].

Despite their potential, widespread adoption of triple-walled carbon nanotubes (TWCNTs) faces significant challenges. Key obstacles include achieving uniform synthesis, addressing characterisation complexities arising from overlapping signals between layers, and gaps in understanding their long-term ecological and biological impacts. While advanced analytical tools such as high-resolution transmission electron microscopy (HRTEM), Raman spectroscopy, and scanning tunnelling microscopy (STM) have enhanced structural and functional analysis, standardised protocols for evaluating TWCNT quality and behaviour remain underdeveloped [11, 12].

This study addresses these challenges through a detailed analytical investigation of TWCNTs' nonlinear vibrational dynamics when embedded in elastic media, employing the homotopy perturbation method (HPM). We

formulate governing equations incorporating geometric nonlinear effects and van der Waals interactions across all three concentric layers. By applying HPM, semi-analytical solutions are derived, focusing on amplitude-frequency relationships and their dependence on material and geometric parameters.

Extensive research has been conducted on the vibration analysis of carbon nanotubes (CNTs) owing to their exceptional mechanical and electromechanical properties, which are critical in nanoscale systems and materials design. Early analytical approaches based on classical beam and shell theories, such as the Euler–Bernoulli and Timoshenko formulations, provided useful insights into fundamental vibration modes of single- and double-walled CNTs but often neglected nanoscale effects. To capture these phenomena more accurately, nonlocal elasticity theory and van der Waals interaction models were developed, accounting for long-range interatomic forces and interlayer coupling. Studies by Wang et al. [13] demonstrated that incorporating these effects leads to size-dependent stiffness and resonance shifts in CNTs.

Despite these advancements, analytical investigations of triple-walled carbon nanotubes (TWCNTs) remain limited. Most existing studies focus on single- or double-walled models, overlooking the distinct tri-layered coupling and nonlinear interlayer interactions that govern TWCNT dynamics. To address this research gap, the present study formulates a three-beam coupled nonlinear vibration model that incorporates geometric nonlinearity and Vander Wall forces among all concentric layers. Using the Homotopy Perturbation Method (HPM), rapidly convergent analytical expressions are derived for vibration amplitudes and frequency responses. This combined analytical–numerical framework not only captures essential nonlinear behaviour and energy transfer mechanisms in TWCNTs but also offers a computationally efficient and physically interpretable approach for modeling nanoscale vibrations.

This paper is structured to address the nonlinear vibrational dynamics of TWCNTs systematically. Section 2 establishes the theoretical framework, deriving governing equations that account for geometric nonlinearities and interlayer van der Waals interactions in TWCNTs. Section 3 outlines applying the homotopy perturbation method (HPM) to solve these equations, emphasising its analytical advantages. Section 4 analyses computational results, elucidating the influence of key parameters—such as elastic medium stiffness and nanotube geometry—on amplitude-frequency responses. Finally, Section 5 synthesises critical findings, highlights practical implications for nanoscale system design, and proposes avenues for future research to address unresolved challenges in TWCNT dynamics.

2. Mathematical Modeling of TWCNT Vibrational Behaviour

Consider a triple-walled carbon nanotube (TWCNT) of length, Young's modulus, density, cross-sectional area, and moment of inertia, embedded in an elastic medium characterised by the foundation stiffness. Each concentric wall of the TWCNT is modeled as a slender, linearly elastic Euler–Bernoulli beam coupled with adjacent walls through van der Waals interactions. The nonlinear vibration behaviour of this system is governed by partial differential equations that incorporate both geometric nonlinearity and interlayer coupling effects.

The governing equation describes the nonlinear transverse vibration of each wall of the TWCNT embedded in an elastic medium. It is derived from the classical Euler–Bernoulli beam theory, incorporating the effects of mid-plane stretching and van der Waals interlayer forces. The equation accounts for material elasticity, foundation stiffness, damping, and interlayer coupling between concentric walls. The nonlinear term arises from geometric nonlinearity in the von Kármán strain relation, representing Duffing-type hardening behaviour. This formulation forms the theoretical basis for analysing amplitude-dependent vibration responses using the Homotopy Perturbation Method (HPM).

Under these assumptions, the nonlinear vibration behaviour of the TWCNT is expressed by the following coupled governing equations:

$$\frac{d^2W_1(t)}{dt^2}+\Big(\frac{\pi^4EI_1}{\rho A_1 l^4}+\frac{c_1}{\rho A_1}\Big)W_1(t)+\frac{\pi^4E}{4\rho l^4}(W_1(t))^3-\frac{c_1}{\rho A_1}W_2(t)=0 \tag{1}$$

$$\frac{d^2W_2(t)}{dt^2}+\Big(\frac{\pi^4EI_2}{\rho A_2 l^4}+\frac{c_1}{\rho A_2}+\frac{c_2}{\rho A_2}\Big)W_2(t)+\frac{\pi^4E}{4\rho l^4}(W_2(t))^3-\frac{c_1}{\rho A_2}W_1(t)-\frac{c_2}{\rho A_2}W_3(t)=0 \tag{2}$$

$$\frac{d^2W_3(t)}{dt^2}+\Big(\frac{\pi^4EI_3}{\rho A_3 l^4}+\frac{c_1}{\rho A_3}+\frac{c_2}{\rho A_3}+\frac{k}{\rho A_3}\Big)W_3(t)+\frac{\pi^4E}{4\rho l^4}(W_2(t))^3-\frac{c_2}{\rho A_3}W_2(t)=0 \tag{3}$$

Here, W_1, W_2, W_3 represent the vibrations of the i^{th} tube along the neutral axis, and c_i denotes the Van der Waals force coefficient between i^{th} and $(i-1)^{th}$ tubes. The governing equations are normalized through the introduction of the following dimensionless parameters:

$$r=\sqrt{\frac{I_1}{A_1}}, x=\frac{W_1}{r}, y=\frac{W_2}{r}, z=\frac{W_3}{r}, \omega_1=\frac{\pi^2}{l^2}\sqrt{\frac{EI_1}{\rho A_1}}, \omega_k=\sqrt{\frac{k}{\rho A_1}},$$
$$\omega_c=\sqrt{\frac{c}{\rho A_1}}, \tau=\omega t, \beta=\frac{A_1}{A_2}, \gamma=\frac{I_1}{I_2}, \eta=\frac{A_1}{A_2}, \zeta=\frac{I_1}{I_3}, \alpha=0.25. \tag{4}$$

By applying a suitable transformation, Equations. (1-3) yield the following dimensionless nonlinear system.

$$\frac{d^2x(\tau)}{d\tau^2}+AB_1x(\tau)+\alpha A(x(\tau))^3-AB_2y(\tau)=0 \tag{5}$$
$$\frac{d^2y(\tau)}{d\tau^2}+AB_1y(\tau)+\alpha A(xy)^3-A\beta B_2x(\tau)-A\beta B_2z(\tau)=0 \tag{6}$$
$$\frac{d^2z(\tau)}{d\tau^2}+AB_4z(\tau)+\alpha A(z(\tau))^3-A\eta B_2z(\tau)=0 \tag{7}$$

where

$$B_1=1+\Big(\frac{\omega_c}{\omega_l}\Big)^2, B_2=\Big(\frac{\omega_c}{\omega_l}\Big)^2, B_3=\beta\Big(\frac{1}{\gamma}+2\Big(\frac{\omega_c}{\omega_l}\Big)^2\Big)$$
$$B_4=\eta\Big(\frac{1}{\zeta}+2\Big(\frac{\omega_c}{\omega_l}\Big)^2+\Big(\frac{\omega_k}{\omega_l}\Big)^2\Big), A=\Big(\frac{\omega_1}{\omega}\Big)^2 \tag{8}$$

It should be noted that the current model is formulated within the context of classical continuum mechanics. At the nanoscale, however, size-dependent or nonlocal effects may play a non-negligible role. A potential extension of this work involves the integration of nonlocal elasticity theory (Eringen 1972)[14], wherein the stress at a point is a function of the strain field across the entire domain. This can be characterised by introducing a nonlocal parameter, defined as $\mu=(e_0a/l)^2$ where e_0 a is a material constant and l is a characteristic length. The incorporation of this parameter would introduce higher-order gradients into the governing equations, a modification expected to manifest as a stiffness-softening effect and a consequent reduction in the system's natural frequencies.
Initial and boundary conditions for the system are specified as follows:

$$x(0)=X_1, y(0)=X_2, z(0)=X_3 \tag{9}$$
$$x'(0)=0, y'(0)=0, z'(0)=0 \tag{10}$$

3. Approximate Analytical solution of String Vibrational Modes Using HPM

Nonlinear phenomena are pervasive across diverse scientific disciplines, particularly in vibration analysis, heat transfer, fluid dynamics, and Nano mechanics—exemplified by challenges such as modeling carbon nanotube vibrations. These systems often involve geometric nonlinearities and coupled interactions, such as Van der Waals forces in multi-walled nanotubes, where numerical methods frequently obscure physical insights due to their inherent complexity. For most such problems, deriving exact analytical solutions remains intractable. Consequently, several approximate analytical methods have been developed, including the Adomian decomposition method [15], variational iteration method [16], Akbari-Ganji method [17, 18], Taylor's Method [19], differential transformation method [20], and the homotopy perturbation method (HPM) [21, 22, 23]. Among these, HPM is the most versatile and efficient approach, applicable to weak and strong nonlinear equations. Demonstrated through extensive studies,

HPM effectively balances accuracy and simplicity, yielding rapidly convergent approximations that closely align with exact solutions, even for highly nonlinear systems. Its adaptability to complex interactions and ability to preserve physical intuition make it indispensable in advancing theoretical and applied research.

The homotopy perturbation method (HPM), pioneered by Ji-Huan He, is a versatile semi-analytical approach for solving nonlinear differential equations. This technique unites classical perturbation theory with topological homotopy concepts, systematically transforming complex nonlinear systems into sequences of simpler linear approximations. Central to HPM is constructing a homotopy equation, which embeds the original nonlinear problem within a continuum of equations governed by a parameter q ∈ [0, 1]. As q evolves from 0 to 1, the homotopy smoothly transitions from an easily solvable linearised form to the complete nonlinear equation, enabling iterative refinement of solutions.

$$x(\tau) = X_1 - \frac{(\alpha X_1^3 + B_1 X_1 - B_2 X_2) A\tau^2}{2} \tag{11}$$

$$y(\tau) = X_2 - \frac{((-X_1 - X_3)\beta B_2 + \alpha X_2^3 + B_3 X_2) A\tau^2}{2} \tag{12}$$

$$z(\tau) = X_3 - \frac{(-\alpha X_3^3 + \eta B_2 X_2 - B_4 X_3) A\tau^2}{2} \tag{13}$$

4. Analytical and Numerical Validation of Carbon Nanotube Vibration Models

The dimensionless vibration of TWCNTs is expressed in Equations (11), (12) and (13), offering a simple analytical form valid for any parameter value. To validate the effectiveness of the proposed HPM approaches, we perform a numerical analysis in this section. The MATLAB-based computational results exhibit high accuracy when compared with the experimental outcomes of this research. The comparative analysis presented in Tables 1,2, 3 featuring both numerical and analytical results along with their average relative errors, establishes the homotopy perturbation method as a precise tool for predicting TWNT vibration amplitudes. The effectiveness of this method is confirmed by the minimal deviations observed, never exceeding 2%.

Table 1. Comparison of theoretical and numerical results of vibration $x(\tau)$ (Equ. 11) using the parameters $\alpha = 0.5, B_1 = 1, B_2 = 1, A = 0.5, X_2 = 1$

	$X_1 = 1$			$X_1 = 1.2$			$X_1 = 1.4$		
τ	NUM	HPM	ERR	NUM	HPM	ERR	NUM	HPM	ERR
0	1	1	0	1.2	1.2	0	1.4	1.4	0
0.2	0.995	0.9952	0.02	1.1894	1.1895	0.01	1.3823	1.3828	0.04
0.4	0.98	0.9816	0.16	1.1574	1.1575	0.01	1.3291	1.3293	0.02
0.6	0.955	0.9551	0.01	1.1042	1.1044	0.02	1.2405	1.2409	0.03
0.8	0.92	0.9204	0.04	1.0297	1.0298	0.01	1.1165	1.1168	0.03
1	0.875	0.876	0.11	0.934	0.9346	0.06	0.957	0.9571	0.01
	Avg Err. %		0.06	Avg Err. %		0.02	Avg Err. %		0.02

Table 2. Thetheoretical and numerical results of vibration $y(\tau)$ (Equ. 12) are examined using the parameters $\alpha = 0.5, \beta = 1, B_1 = 1, B_2 = 1, B_3 = 1, X_1 = 1$

	$X_2 = 1$			$X_2 = 1.05$			$X_2 = 1.10$		
τ	NUM	HPM	ERR	NUM	HPM	ERR	NUM	HPM	ERR
0	1	1	0	1.05	1.05	0	1.1	1.1	0
0.2	1.005	1.0098	0.48	1.0537	1.0538	0.01	1.103	1.1062	0.29
0.4	1.02	1.0245	0.44	1.0649	1.0652	0.03	1.1094	1.113	0.32
0.6	1.045	1.0489	0.37	1.0834	1.0838	0.04	1.1211	1.1241	0.27
0.8	1.08	1.083	0.28	1.1094	1.1096	0.02	1.1375	1.1397	0.19
1	1.125	1.1269	0.17	1.1428	1.143	0.02	1.1586	1.1598	0.10
	Avg Err. %		0.29	Avg Err. %		0.02	Avg Err. %		0.20

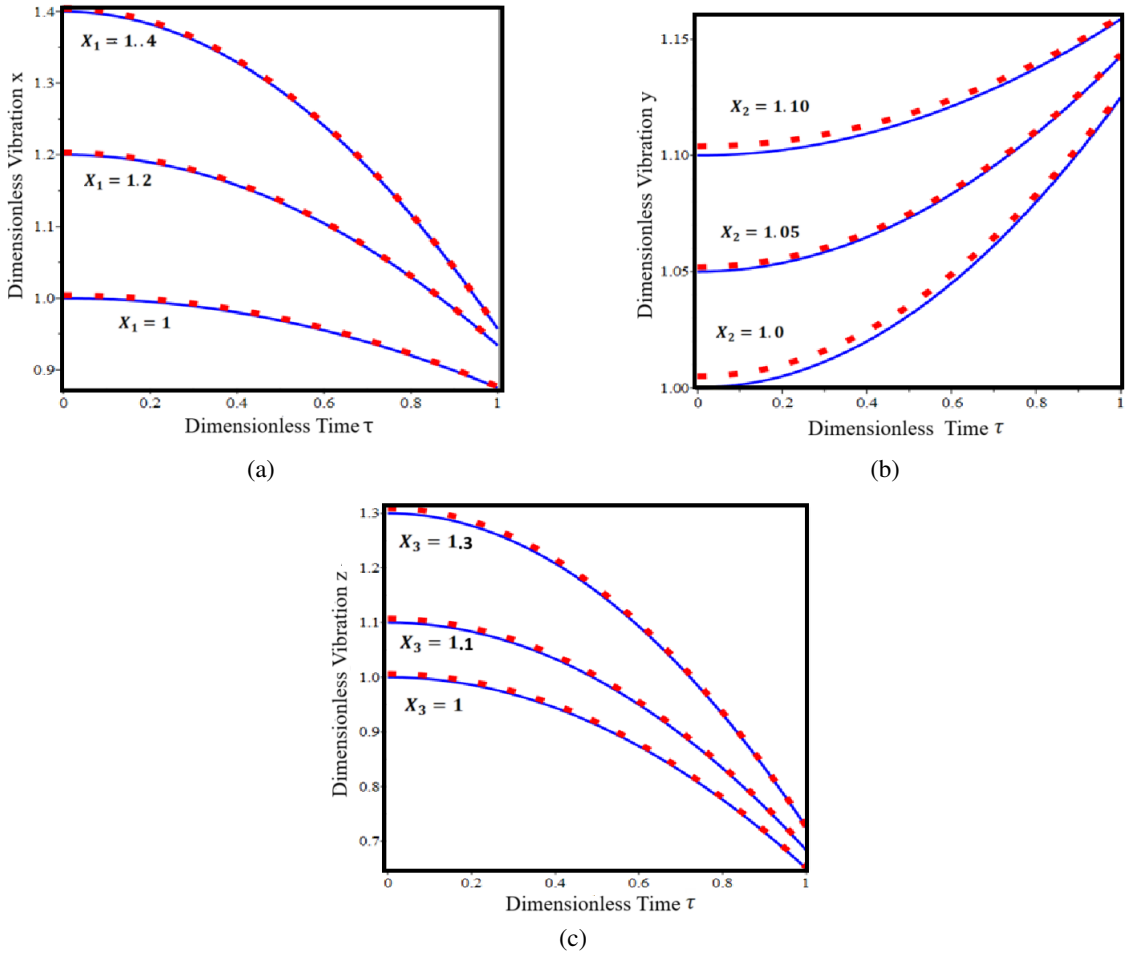

Figure 1. Variation of dimensionless vibration x with dimensionless time τ parameter values $\alpha, \beta, \eta, A, B_1, B_2, B_3, X_1, X_2, X_3$ as calculated from Equation (11). The geometric parameters used in this analysis are $\alpha = 0.5, \beta = 1, \eta = 0.1, B_1 = 1, B_2 = 1, B_3 = 1, X_1 = 1, X_2 = 1, X_3 = 1$

Table 3. Theoretical versus numerical results of vibration $x(\tau)$ (Equ. 13) using the parameters $\alpha = 0.5, \beta = 1, \eta = 0.1, B_1 = 1, B_2 = 1, B_3 = 1, X_1 = 1, X_2 = 1$

	$X_3 = 1$			$X_3 = 1.1$			$X_3 = 1.3$		
τ	NUM	HPM	ERR	NUM	HPM	ERR	NUM	HPM	ERR
0	1	1	0	1.1	1.1	0	1.3	1.3	0
0.2	0.986	0.9968	1.10	1.0833	1.0837	0.04	1.277	1.2857	0.68
0.4	0.944	0.9448	0.08	1.0334	1.0347	0.13	1.2081	1.2158	0.64
0.6	0.874	0.875	0.11	0.9501	0.9521	0.21	1.0931	1.0993	0.57
0.8	0.776	0.78	0.52	0.8335	0.8347	0.14	0.9322	0.9361	0.42
1	0.65	0.6512	0.18	0.6836	0.6844	0.12	0.7254	0.7264	0.14
	Avg Err. %		0.33	Avg Err. %		0.11	Avg Err. %		0.41

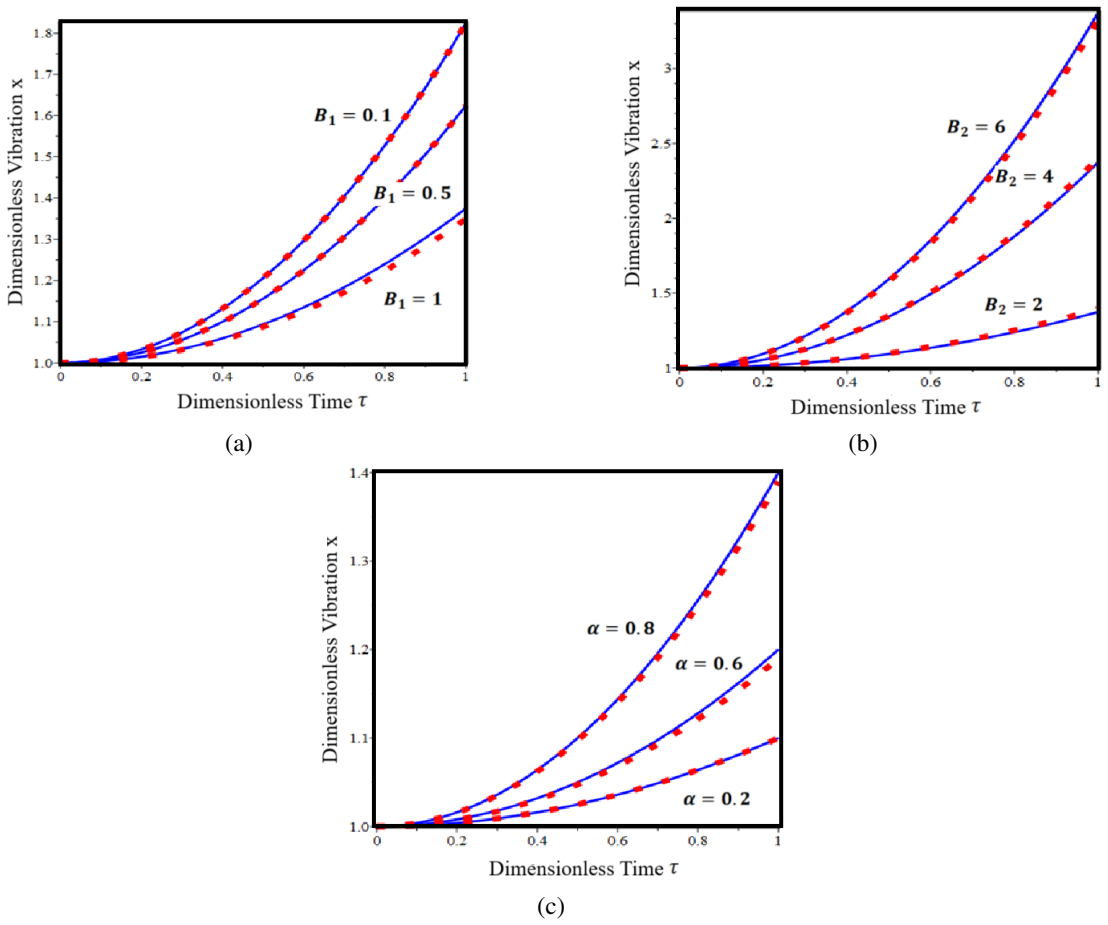

Figure 2. Showing the dimensionless vibration amplitude $x(\tau)$ plotted against dimensionless time tau for various parameter values $\alpha, \beta, \eta, A, B_1, B_2, B_3, X_1, X_2, X_3$ as calculated from Equation (11). The geometric parameters used in this analysis are $\alpha = 0.2, \beta = 1, \eta = 0.1, B_1 = 0.1, B_2 = 2, B_3 = 1, X_1 = 1, X_2 = 1, X_3 = 1$

4.1. Findings and Interpretations

Figures 1(a)–(c) illustrate the temporal evolution of the dimensionless displacements of the three concentric nanotube walls under identical normalised loading.

Figure 1(a) shows a gradual decay with time. This attenuation arises from two primary effects: (i) the linear foundation stiffness, which provides a restoring force proportional to displacement, and (ii) the energy-dissipative contribution associated with the damping coefficient in the non-dimensional formulation. At higher initial amplitudes, the nonlinear geometric term transiently stiffens the response, producing larger initial oscillations before the same restoring and dissipative terms govern the decay.

Figure 1(b) increases with time, whereas decay. This seemingly counterintuitive trend originates from nonlinear interlayer coupling. The middle wall interacts with both the inner and outer walls through van der Waals forces; as a result, a portion of the energy initially stored in the outer or inner walls is transferred to the middle wall. Two mechanisms contribute to this behaviour: (i) mode coupling, in which near-resonance between coupled natural frequencies facilitates energy exchange; and (ii) nonlinear frequency modulation caused by the cubic stiffness term, which shifts the instantaneous frequencies and promotes transient energy localisation in the middle layer. Thus, the observed growth is fully consistent with the coupled nonlinear dynamics predicted by the model.

Figure 1(c) reveals that it follows a decay pattern similar to that of, again reflecting the combined influence of the restoring stiffness and damping terms. The amplitude dependence is governed by the nonlinear stiffness, which increases the effective stiffness at larger deflections.

Figures 2(a)–(c) illustrate the dynamic behaviour of the dimensionless vibration response over the dimensionless time, highlighting the sensitivity of the system to variations in the parameters, and the fractional-order parameter, respectively. These plots serve to validate the numerical model by comparing it (red dot) with the analytical solution (blue line).

Figure 2(a) illustrates the effect of the stiffness parameter on the dimensionless vibration amplitude of the inner wall of the triple-walled carbon nanotube as a function of dimensionless time. It is observed that as the amplitude increases, the amplitude of vibration decreases for a given time, indicating that higher stiffness in the innermost wall results in greater resistance to radial expansion.

Figure 2(b) shows the influence of the intermediate wall stiffness parameter on the dynamic response of the inner tube. An increase in leads to a significant rise in the amplitude of vibration, suggesting a strong coupling effect between the walls. This behaviour underscores the sensitivity of the inner tube's motion to the mechanical characteristics of the middle layer in TWCNTs.

Figure 2(c) demonstrates the effect of the van der Waals interaction parameter on the dimensionless vibration response of the inner wall. As the vibration amplitude increases, the vibration amplitude becomes more pronounced, signifying that stronger interlayer van der Waals forces amplify the mechanical energy transfer across the layers, thereby increasing the inner tube's response.

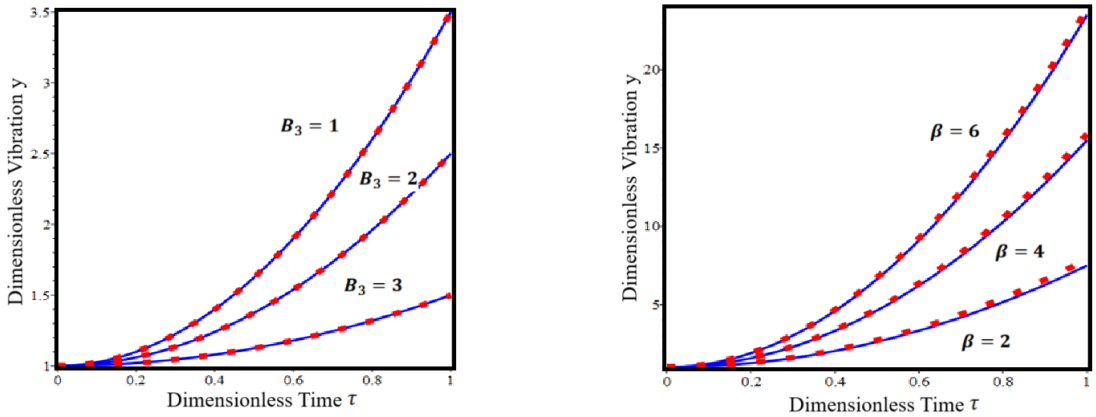

(a) (b)

Figure 3. Showing the dimensionless vibration response $y(\tau)$ versus dimensionless time τ for various parameter combinations $\alpha = 0.25, \beta = 1, \eta = 1, B_1 = 2, B_2 = 1, B_3 = 1, X_1 = 1, X_2 = 1, X_3 = 1$ as calculated as Eq.(13)

Figure 3a illustrates the influence of the dimensionless parameter on the dimensionless transverse vibration of triple-walled carbon nanotubes as a function of dimensionless time. The parameter may be associated with the stiffness or interaction coefficient between the concentric walls of the TWCNT. It is observed that increasing the value of leads to a significant decrease in the amplitude of vibration. This behaviour can be attributed to the enhanced mechanical coupling between the nanotube walls, which imposes additional resistance to deformation, thus attenuating the vibratory response over time.

Figure 3b presents the effect of the external loading parameter on the dimensionless vibration. A rise in results in a pronounced increase in vibration amplitude, demonstrating the sensitivity of the nanotube's dynamic response to external excitations. The curves indicate a nonlinear growth in vibration as the load increases, highlighting the importance of considering loading intensity in the design and application of TWCNT-based nanoelectromechanical systems (NEMS). This behaviour emphasises the critical role of external excitation in determining the operational stability of TWCNTs under dynamic environments.

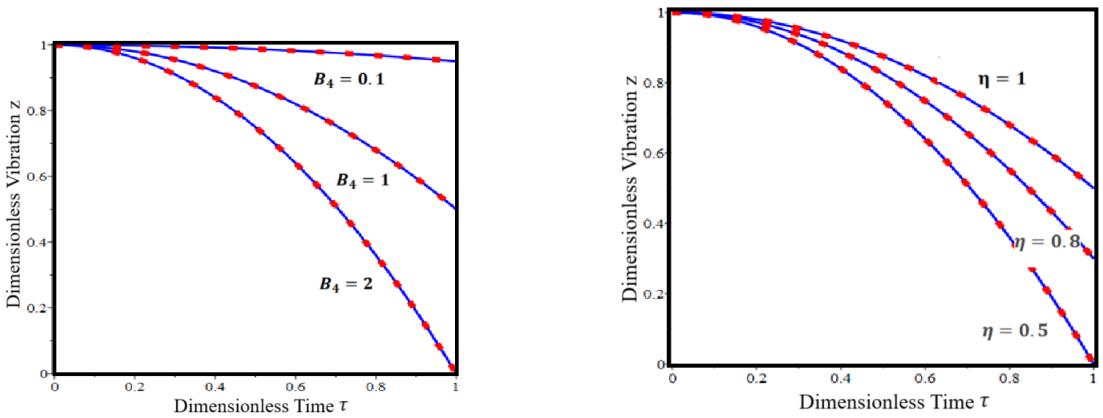

Figure 4. Figure showing the dimensionless vibration response $z(\tau)$ versus dimensionless time τ for various parameter combinations $\alpha = 2, \beta = 1, \eta = 0.5, B_1 = 2, B_2 = 1, B_3 = 1, B_4 = 0.1, X_1 = 1, X_2 = 1, X_3 = 1$ as calculated as Eq.(13)

Figure 4(a-b) presents the variation of the dimensionless vibration amplitude as a function of the dimensionless time, highlighting the influence of both the viscous damping parameter and the fractional derivative order η.

Figure 4a illustrates the impact of the damping parameter on the system's dynamic response. Results are depicted for. It is observed that increasing significantly accelerates the attenuation of vibration amplitudes, indicating enhanced energy dissipation. This trend aligns with classical damping theory, where higher damping coefficients lead to faster decay of oscillations. The numerical (red dot) and analytical (blue lines) results show excellent agreement, thereby confirming the accuracy of the proposed model.

Figure 4b shows the response of the system for different values of the fractional order. The results reveal that higher values correspond to a slower decay of the vibration amplitude, signifying a weaker damping effect. This behaviour reflects the inherent memory characteristics of fractional viscoelastic materials: as increases, the system retains more of its past behaviour, resulting in slower energy dissipation. The use of fractional-order derivatives in modeling thus enables a more flexible and accurate representation of complex damping behaviour in viscoelastic media.

5. Conclusion

The present research employed the Homotopy Perturbation Method (HPM) to examine the nonlinear vibration response of triple-walled carbon nanotubes (TWCNTs) embedded in an elastic medium. The derived first-order analytical solution exhibits rapid convergence and shows excellent agreement with numerical simulations,

demonstrating the reliability and efficiency of the proposed formulation. The results indicate that the outer and inner walls undergo amplitude decay primarily due to restoring and damping effects, whereas the middle wall displays a transient increase in displacement attributed to nonlinear interlayer energy transfer. The analysis further highlights that variations in foundation stiffness, damping coefficient, and van der Waals coupling parameters significantly influence the vibration amplitude, frequency modulation, and dynamic energy redistribution within the TWCNT system.

Although the present formulation provides clear physical insight and analytical accuracy, it remains subject to certain limitations. The study assumes linear foundation behaviour, integer-order damping, and neglects temperature-dependent and viscoelastic effects, which may influence large-amplitude or high-frequency responses. Future research should extend the present model by incorporating higher-order HPM approximations, fractional damping and nonlocal elasticity theories, as well as experimental and molecular dynamics validations. Such advancements would strengthen the predictive capability of the analytical framework and enhance its applicability to the design and optimisation of nanoscale mechanical systems in engineering and materials science.

Nomenclature

ω	- Nonlinear free vibration frequency (cm^{-1})
k	- Spring Constant (N/m^2)
ρ	- Density (kg/m^3)
A_1, A_2, A_3	- Cross Section Area $(nm)^2$
E	- Young Modulus $(TP\alpha)$
I_1, I_2, I_3	- Crosss sectional inertia moment $(TP\alpha)$
W_1, W_2, W_3	- Transverse displacement of the i^{th} tube on the neutral axis $(TP\alpha)$
t	- Time (s)
l_1, l_2, l_3	- Length oof TWNT (nm)
$\omega_c, \omega_k, \omega_l$	- Dimensionaless Constant
X	- Dimensionless Vibration amplitude
$\alpha, \beta, \gamma, \eta, \zeta$	- Dimensionless constant
τ	- Dimensionless Time
x, y, z	- Dimensionless Vibration amplitude
r	- Dimensionless variable

Appendix A

The homotopy for the equation (5) to (7) as follows

$$(1-p)\Big(\frac{d^2x(\tau)}{d\tau^2}\Big) + p\Big(\frac{d^2x(\tau)}{d\tau^2} + AB_1x(\tau) + \alpha A(x(\tau))^3 - AB_2y(\tau)\Big) = 0 \tag{14}$$

$$(1-p)\Big(\frac{d^2y(\tau)}{d\tau^2}\Big) + p\Big(\frac{d^2y(\tau)}{d\tau^2} + AB_2y(\tau) + \alpha A(y(\tau))^3 - A\beta B_2x(\tau) - A\beta B_2z(\tau)\Big) = 0 \tag{15}$$

$$(1-p)\Big(\frac{d^2z(\tau)}{d\tau^2}\Big) + p\Big(\frac{d^2x(\tau)}{d\tau^2} + AB_4z(\tau) + \alpha A(z(\tau))^3 - A\eta B_2z(\tau)\Big) = 0 \tag{16}$$

The approximate outcomes of (14) to (16) are

$$x = x_0 + px_1 + p^2x_2 + ... \tag{17}$$

$$y = y_0 + py_1 + p^2y_2 + ... \tag{18}$$

$$z = z_0 + pz_1 + p^2z_2 + ... \tag{19}$$

Substituting equation (17) into (14) and comparing the coefficient of like powers of p

$$p^0 : \frac{d^2x_0(\tau)}{d\tau^2} = 0; \frac{dx_0(\tau)}{d\tau^2} = 0, x_0(0) = X_1 \tag{20}$$

$$p^1 : \Big(\frac{d^2x_1(\tau)}{d\tau^2} + AB_1x(\tau) + \alpha A(x(\tau))^3 - AB_2y(\tau)\Big) = 0; \frac{dx_1(\tau)}{d\tau} = 0, x_1(0) = 0 \tag{21}$$

$$p^0 : \frac{d^2y_0(\tau)}{d\tau^2} = 0; \frac{dy_0(\tau)}{d\tau^2} = 0, y_0(0) = X_2 \tag{22}$$

$$p^1 : \Big(\frac{d^2y_1(\tau)}{d\tau^2} + AB_2y(\tau) + \alpha A(y(\tau))^3 - A\beta B_2x(\tau) - A\beta B_2z(\tau)\Big) = 0; \frac{dy_1(\tau)}{d\tau} = 0, y_1(0) = 0 \tag{23}$$

$$p^0 : \frac{d^2z_0(\tau)}{d\tau^2} = 0; \frac{dz_0(\tau)}{d\tau^2} = 0, z_0(0) = X_3 \tag{24}$$

$$p^1 : \Big(\frac{d^2z_1(\tau)}{d\tau^2} + AB_4z(\tau) + \alpha A(z(\tau))^3 - A\eta B_2z(\tau)\Big) = 0; \frac{dz_1(\tau)}{d\tau} = 0, z_1(0) = 0 \tag{25}$$

By resolving equation (20) and (21) the following result can be obtained

$$x_0(\tau) = X_1 \tag{26}$$

$$x_1(\tau) = \frac{-(\alpha X_1^3 + B_1X_1 - B_2X_2)A\tau^2}{2} \tag{27}$$

$$x = lim_{p\to 1}x = x_0 + x_1 \tag{28}$$

$$x = X_1 - \frac{(\alpha X_1^3 + B_1X_1 - B_2X_2)A\tau^2}{2} \tag{29}$$

Similarly the approximate solution for equation (6) and (7) can be derived.

REFERENCES

1. Iijima, S., *Helical microtubules of graphitic carbon*, Nature, 354(6348 (1991)), 56-58.
2. Endo, M., Strano, M. S., & Ajayan, P. M., *Potential applications of carbon nanotubes*, Topics in Applied Physics, 111 (2005), 13–61.
3. Zhang, Y., Wang, Y., & Jia, Y., *Triple-walled carbon nanotubes: A potential reinforcement for polymer nanocomposites*, Composites Science and Technology, 72(14) (2012), 1559–1565.
4. Xu M, Futaba DN, Yamada T, Yumura M, Hata K, *Carbon nanotubes with temperature-invariant viscoelasticity from -196 degrees to 1000 degrees C*, Science, 330(6009)(2010) 1364-8. doi: 10.1126/science.1194865.
5. Dresselhaus, M. S., & Avouris, P. , *Introduction to carbon materials research. In Carbon nanotubes: synthesis, structure, properties, and applications*, (2001) (pp. 1-9). Berlin, Heidelberg: Springer Berlin Heidelberg.
6. Tasis, D., Tagmatarchis, N., Bianco, A., & Prato, M., *Chemistry of carbon nanotubes*, Chemical Reviews, 106(3), (2006) 1105–1136.
7. Zhang, M., Yudasaka, M., & Iijima, S., *A novel synthesis method for triple-walled carbon nanotubes*, Chemical Physics Letters, 422(4–6) (2007), 575–580.
8. Popov, V. N., Lambin, P., & Henrard, L., *Theoretical Raman intensity of the radial breathing mode of single-walled carbon nanotubes*, Nano Letters, 2(9) (2002), 1103–1106.
9. Wang, C., Li, D., Too, C. O., & Wallace, G. G., *Electrochemical properties of aligned carbon nanotube arrays*, Chemical Society Reviews, 42(7 (2013)), 2910–2930.
10. Liu, Z., Tabakman, S., Welsher, K., & Dai, H., *Carbon nanotubes in biology and medicine: In vitro and in vivo detection, imaging and drug delivery*, Nano Research, 2(2) (2009), 85–120.
11. Fantini, C., Jorio, A., Souza, M., Strano, M. S., Dresselhaus, M. S., & Pimenta, M. A., *Optical transition energies for carbon nanotubes from resonant Raman spectroscopy: Environment and temperature effects*, Physical Review Letters, 93(14)(2004), 147406.
12. Y.D. Kuang, X.Q. He , C.Y. Chen , G.Q. Li, *Analysis of nonlinear vibrations of double walled carbon nanotubes conveying fluid*, Computational Materials Science 45 (2009) 875–880
13. Wang, C. M., Zhang, Y. Y., Ramesh, S. S., & Kitipornchai, S. *Buckling analysis of micro-and nano-rods/tubes based on nonlocal Timoshenko beam theory*, Journal of Physics D: Applied Physics, 39(17), 3904, (2006).
14. Eringen, A. C., & Edelen, D, *On nonlocal elasticity*, International journal of engineering science, 10(3), 233-248, (1972).
15. Zeidan D, Chau CK, Lu TT. *On the characteristic Adomian decomposition method for the Riemann problem*, Math Method Appl Sci.; 44 (2021), 8097–8112. http://dx. doi.org/10.1002/mma.5798
16. J. H. He, Xu-Hong Wu, *Variational iteration method: New development and applications*, Comput. Math. with Appl., 54 (2007) 881–894

17. Nebiyal, A., R. Swaminathan, and S. G. Karpagavalli, *Reaction kinetics of amperometric enzyme electrode in various geometries using the Akbari-Ganji method*, International Journal of Electrochemical Science, 18(9) (2023): 100240.
18. Akbari MR, Ganji DD, Majidian A, Ahmadi AR, *Solving nonlinear differential equations of Vanderpol, Rayleigh and Duffing by AGM*, Front Mech Eng. 9 (2014) 177–190.
19. Rajalakshmi, R., Rajendran, L., & Naganathan, S., *Exploring Nonlinear Reaction Kinetics in Porous Catalysts: Analytical and Numerical Approaches to LHHW Model*, Statistics, Optimization & Information Computing, 2025.
20. Raja, R., and R. Swaminathan, *Mathematical Analysis of Nonlinear Differential Equations in Polymer Coated Microelectrodes*, Contemporary Mathematics(2024), 2569-2582.
21. J He JH., *Homotopy perturbation method: A new nonlinear analytical technique*, Appl Math Comput. 135(1) (2003), 73–79. http://dx.doi.org/10.1016/S0096 3003(01)00312-5.
22. Swaminathan, R., Saravanakumar, R., Venugopal, K., & Rajendran, L, *Analytical solution of nonlinear problems in homogeneous reactions occur in the mass-transfer boundary layer: homotopy perturbation method*, International Journal of Electrochemical Science, 16(6) (2021), 210644.
23. Raju, R. Vignesh, R. Swaminathan, M. C. Kekana, N. Jeeva, and S. E. Fadugba, *Analytical techniques for understanding biofilm modeling in indoor air quality management* Results in Control and Optimization (2025): 100564.